

# Grain boundary embrittlement in Cu–Al–Ni $\beta$ -phase alloys

S. W. HUSAIN, M. AHMED

*Dr A.Q.Khan Research Laboratories, Kahuta, GPO Box 502, Rawalpindi, Pakistan*

P. C. CLAPP

*Department of Metallurgy, University of Connecticut, Storrs, Connecticut 06268, USA*

The grain boundary embrittlement in Cu–Al–Ni  $\beta$ -phase alloys has been investigated. The study included both the bulk alloys and rapidly solidified ribbons. It was observed that the fracture characteristics and the phase transformations in rapidly solidified ribbons were similar to those in the bulk alloys. Various factors responsible for intergranular fracture were considered. It was found that intrinsic or extrinsic precipitates at the grain boundaries are not responsible for the embrittlement. It was further observed that the segregation of impurities does not occur at the grain boundaries and hence is not a factor contributing to the embrittlement. The intrinsic characteristics, however, appear to play an important role. These may include high elastic anisotropy, ordered structure and plastic incompatibility. Severe embrittlement in high-nickel alloys is associated with spinodal decomposition occurring in these alloys. The large grain size exhibited by these alloys is found not to be a significant factor contributing to the embrittlement.

## 1. Introduction

Cu–Al–Ni  $\beta$ -phase alloys have received considerable attention in recent years because of their excellent shape memory properties [1]. In addition they have good corrosion resistance and high hardness and strength. Unfortunately these alloys exhibit poor impact strength. The brittleness of these alloys is associated with intergranular fracture. The composition of general interest is 14 wt % Al with a varying nickel content. The brittleness increases with increasing nickel content, and at compositions near 10 wt % Ni the alloys become so brittle that they sustain intergranular cracks when quenched from solution-treatment temperature [2]. The extreme brittleness observed in Cu–14 wt % Al–10 wt % Ni alloy was the main reason for selecting this composition for the present investigation. In order to facilitate a better understanding of the various phases and the phase transformations involved, a section of the Cu–Al–Ni ternary phase diagram is presented in Fig. 1 [3]. The phases that form in the region of interest are described in Table I. The table contains two additional phases,  $\beta_1$  and martensite, which are not present in the equilibrium phase diagram. During the study of phase transformations in Cu–14 wt % Al–10 wt % Ni alloys it was observed that quenching in cold water results in the ordering of  $\beta$  phase forming  $\beta_1$  phase [2]. The samples quenched in boiling water or those cooled in air form martensite. This behaviour, i.e. martensitic transformation occurring at slower cooling rates, is in contrast to the normal observation where martensitic transformation occurs at relatively faster cooling rates. This is due to the precipitation of NiAl phase during the cooling cycle. The depletion of nickel in the matrix raises the

$M_s$  temperature values higher than room temperature. In the present investigation, the emphasis is on the properties of alloys containing  $\beta_1$  phase since they are more important from the application point of view.

The present work examines the experimental evidence in regards to the possible mechanisms associated with the intergranular embrittlement in Cu–Al–Ni  $\beta$ -phase alloys. Theoretical considerations for the latter have also been explored.

## 2. Experimental procedures

The alloys of Cu–14 wt % Al–10 wt % Ni composition were prepared in a controlled-atmosphere induction furnace using copper (99.99%), nickel (99.99 + %) and aluminium (99.999%). The samples were melted in an argon gas atmosphere and then cast into a copper mould. The castings were homogenized for 4 h at 950°C and air-cooled. The samples were solutionized at 950°C for 45 min and cooled in the desired medium (iced brine, boiling water and air). After homogenization the composition of the alloys was checked using wet chemical analysis and the impurity content was determined using a mass spectrometer. The samples for Auger electron spectroscopic analysis were broken inside the vacuum chamber of the spectrometer and the freshly fractured grain boundary surfaces were analysed. Homogenized alloy was used to make thin ribbons of rapidly solidified material using a melt-spinning technique. The samples were induction-melted under an argon atmosphere and a jet of molten alloy was ejected on to a 15 cm diameter copper wheel rotating at a speed of 5000 r.p.m. The melt-spinning produced ribbons approximately 5 mm wide and 10 to 50  $\mu$ m thick. Thin foils for transmission electron

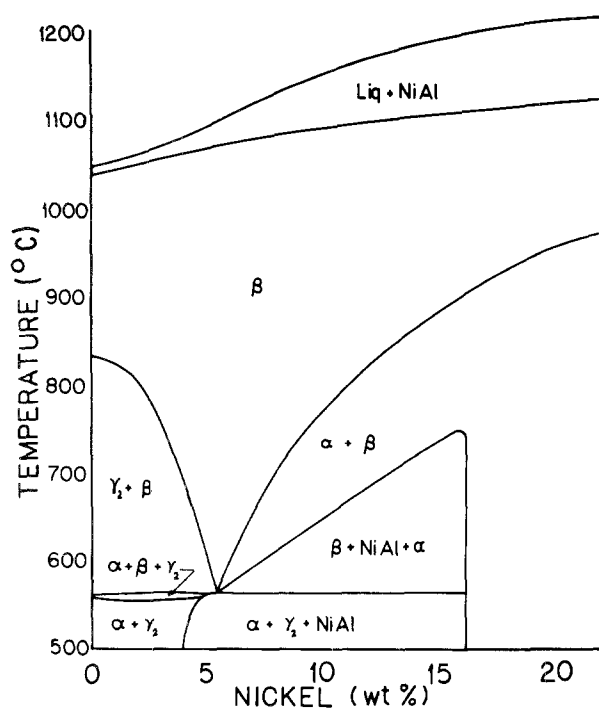


Figure 1 Cu–Al–Ni phase diagram, section taken at 14 wt% Al, after Alexander [3] (note: Alexander used the symbol  $\delta$  instead of  $\gamma_2$ ).

microscopy were prepared using 1:3 nitric acid in methanol at  $-55^\circ\text{C}$ .

### 3. Results and discussion

Cu–Al–Ni  $\beta$ -phase alloys exhibit brittle intergranular fracture under ambient conditions (i.e. room temperature and ordinary atmospheric conditions). The embrittlement is manifested in both tensile and impact tests. A typical fracture surface observed in specimens subjected to impact test is shown in Fig. 2. These features rule out the possibility of hydrogen embrittlement and stress–corrosion cracking. Therefore the reasons for such embrittlement may include precipitation at the grain boundaries, segregation of impurities at the grain boundaries, elastic and plastic incompatibilities and certain types of phase transformations. Large grain size is also known to aggravate the problem. The reasons outlined above will now be discussed separately in the light of experimental evidence in regards to the Cu–Al–Ni  $\beta$ -phase alloys.

#### 3.1. Grain boundary precipitates

The intergranular fracture can result either due to intrinsic or extrinsic precipitates along the grain boundaries. In the Cu–Al–Ni system, a brittle phase

TABLE I Phases present in the  $\beta$ -phase region

Phase	Description
$\alpha$	Primary solid solution of aluminium and nickel in copper, fcc structure
$\beta$	High-temperature disordered phase based on $\text{Cu}_3\text{Al}$ , bcc structure
$\beta_1$	Low-temperature ordered phase based on $\text{Cu}_3\text{Al}$ , $\text{DO}_3$ structure
$\gamma_2$	Complex cubic structure
Martensite	Ordered phase with orthorhombic structure
NiAl	Ordered bcc structure

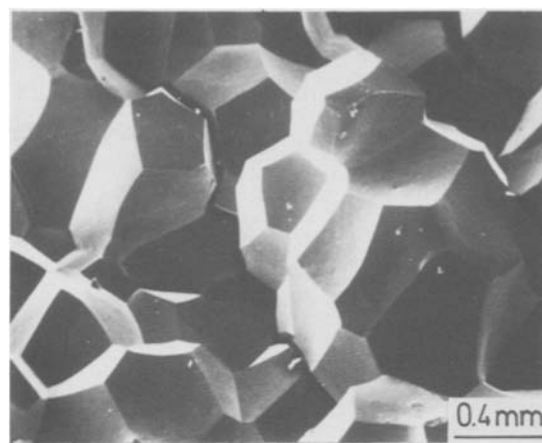


Figure 2 Scanning electron micrograph showing intergranular fracture observed in as-quenched samples.

$\gamma_2$  can precipitate intrinsically in accordance with the phase equilibrium. Precipitation along the grain boundaries can also occur extrinsically, i.e. by incorporating some impurities during processing. In particular, the oxygen pick-up can lead to oxide formation along the grain boundaries and thereby make them brittle. In the following paragraphs we will examine both the direct and indirect evidence regarding the role of grain boundary precipitates in the embrittlement.

The alloys studied have a single-phase structure above  $830^\circ\text{C}$ . The solution treatment is normally carried out at temperatures near  $900^\circ\text{C}$ . To eliminate the possibility of any  $\gamma_2$  phase persisting at the grain boundaries some samples were solution-treated for up to 40 h at  $1020^\circ\text{C}$  (close to the solidus temperature which is about  $1050^\circ\text{C}$ ). The samples after this treatment were quenched directly into iced brine. The fracture of all such samples was completely intergranular. The fracture remained completely intergranular irrespective of the cooling medium. The latter included iced brine, boiling water and air. Such a behaviour suggests that precipitation along grain boundaries is not responsible for the embrittlement. Further, the experimental evidence including Auger electron spectroscopy indicated that the role of oxygen in this embrittlement was insignificant. This aspect has been discussed in detail elsewhere [4].

As far as direct observation is concerned, the grain boundaries examined using optical and scanning electron microscopy did not show any precipitation. The transmission electron microscopic examination of the grain boundary region was difficult because of the large grain size in these alloys (of the order of 1 mm). The thinned specimens normally perforated in regions contained within the grain. In order to improve the chances of getting grain boundaries in the thinned area, a rapid solidification technique was utilized to get thin ribbons. The grain size in this material was of the order of few micrometres. The fracture of these ribbons was also intergranular (except in some regions having very small equiaxed grains where the fracture was predominantly transgranular). An electron micrograph obtained from these ribbons is represented in Fig. 3a. It can be seen that the grain boundaries lack

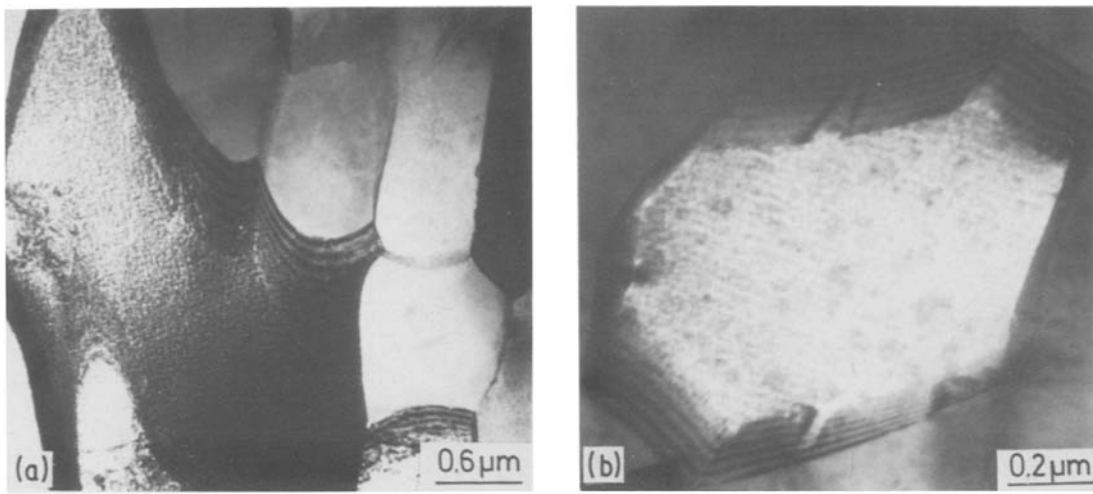


Figure 3 Bright-field transmission electron micrographs obtained from rapidly solidified ribbon: (a) bright-field image showing randomly oriented grains, (b) thickness contours along the grain boundaries.

evidence of any precipitation. This was further established by observing the specimens at higher magnifications and at various tilt angles. Regular thickness contours also suggested the absence of second-phase particles at the grain boundaries (Fig. 3b). This suggests that grain boundary precipitates, whether intrinsic or extrinsic, are not responsible for the intergranular embrittlement in these alloys.

### 3.2. Grain boundary segregation

In recent years most of the cases of intergranular fracture have been found to be associated with the segregation of impurities at the grain boundaries [5]. Various impurities are known to cause intergranular weakness in copper-based alloys, of which bismuth and antimony are the most harmful [6]. In the present investigation, mass spectroscopic analysis carried out to establish the impurity content within the bulk alloy showed that the concentration of harmful impurities (such as arsenic, tin, antimony, bismuth and lead) was less than 2 p.p.m. These levels are quite low to cause any significant concentration of impurities at the grain boundaries. This was further checked by Auger electron spectroscopic analysis. No impurity segregation was detected at the grain boundary fracture surfaces in the Auger analysis [4]. As mentioned earlier, even those alloys which were solution-treated close to the solidus temperature and quenched directly into iced brine showed completely intergranular fracture. Such observations are contrary to what would be expected if the embrittlement were due to impurity segregation. At such high temperatures the impurities are likely to be distributed uniformly rather than segregated at the grain boundaries.

### 3.3. Elastic anisotropy

Incompatibility stresses are introduced at the grain boundaries because of elastic anisotropy [7]. The magnitude of this stress concentration increases as the elastic anisotropy increases. The extent of elastic anisotropy is usually represented by the ratio of elastic constants [8]

$$A = 2C_{44}/(C_{11} - C_{12})$$

The value of the anisotropy factor  $A$  has been reported to be 13 for Cu–14.0 wt % Al–4.2 wt % Ni alloy [9], showing that these alloys are highly anisotropic. Unfortunately, values of the anisotropy factor are not available for higher-nickel alloys which are even more brittle. To investigate the role of elastic anisotropy, Miyazaki *et al.* [10] have studied in detail the deformation behaviour of bicrystals of Cu–14.6 wt % Al–4 wt % Ni alloy. They found that the random bicrystals fractured at low stresses ( $\sim 100$  MPa) without any plastic deformation and the fracture path was intergranular. The symmetric bicrystals fractured at significantly higher stresses ( $\sim 600$  MPa) with about 30% elongation and the fracture path was transgranular. The difference in fracture behaviour was attributed to the presence (or absence) of stress concentration at the grain boundaries due to elastic anisotropy.

### 3.4. Plastic incompatibility

As pointed out by Von Mises [11], in the absence of any other mode of plastic deformation, five independent slip systems are required to produce a general, homogeneous strain without any change in volume. The deformation of a polycrystalline solid can proceed without the formation of voids or cracks at the grain boundaries only when the grains can undergo a general strain. When five independent slip systems are not available, the formation of cracks is usually observed [12]. There are many intermetallics and ionic compounds which fail to satisfy this condition and exhibit intergranular fracture [13].

The  $\beta$ -phase in the Cu–Al–Ni system has a  $DO_3$  structure in the quenched condition. It has been suggested that the  $DO_3$  structure should have a  $\{110\} \langle 111 \rangle$  type of slip system [14]. This incorporates five independent slip systems. The actual operative slip systems, however, depend not only on the crystal structure but also on the relative energy of various dislocation configurations. This is specially true for alloys which show high elastic anisotropy [15]. It is, therefore, necessary to find the operative slip systems before drawing any conclusion about their role in the brittleness of these alloys. It should be noted that

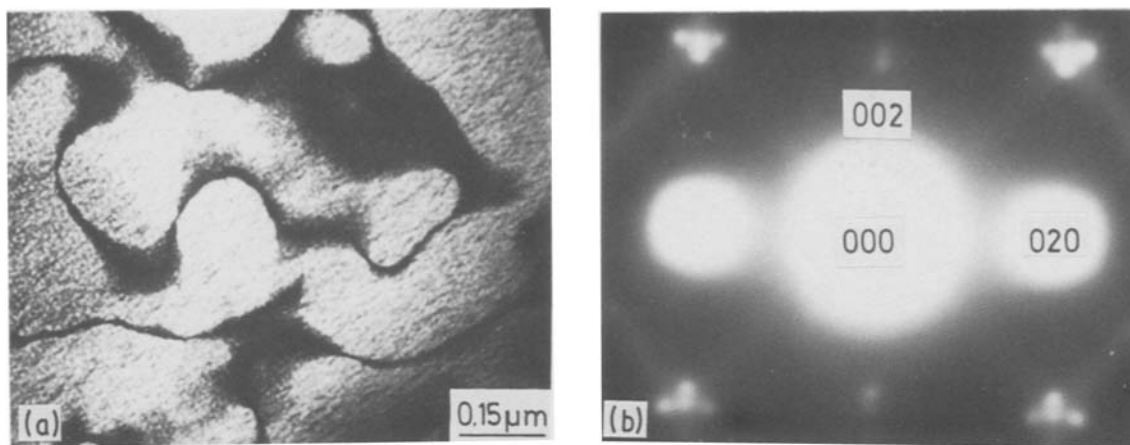


Figure 4 TEM information obtained from rapidly solidified ribbons: (a) dark-field image formed using 020 type superlattice spot, (b) the corresponding diffraction pattern.

the number of independent slip systems required for deformation of a symmetric bicrystal is less than in the case of a random bicrystal. Thus the observations of Miyazaki *et al.* [10] may also be explained in terms of the plastic incompatibility in these alloys.

### 3.5. Ordered structure

Alloys with an ordered structure are in general brittle. In most cases the fracture is intergranular. Some of the ordered alloys known to exhibit intergranular fracture are NiAl [16], Ni<sub>3</sub>Al [17], FeAl [18], Fe<sub>3</sub>Al [19] and FeCo [20]. As pointed out by Marcinkowski [21], two probable reasons for this behaviour are (a) the relatively high energy of the grain boundaries in ordered alloys as compared to disordered alloys, and (b) the difficulty of cross-slip in ordered alloys which makes strain accommodation at the grain boundaries difficult.

The high-temperature  $\beta$ -phase in Cu–Al–Ni alloys possesses a disordered bcc structure. The  $\beta$ -phase orders during quenching to form  $\beta_1$  phase having a DO<sub>3</sub> type structure [22]. The ordered structure may be playing a role in the intergranular embrittlement of these alloys. However, the relative contribution of ordering can be determined only when the fracture behaviour of the disordered and ordered state are compared. Unfortunately it is not possible in these alloys, since they become ordered even when prepared using a spin-quenching technique where the cooling rate during solidification is of the order of  $10^6$  °C sec<sup>-1</sup>. This is shown in Fig. 4, where anti-phase domains are seen in the dark-field image and the associated diffraction pattern corresponds to a DO<sub>3</sub>-type structure.

### 3.6. Spinodal decomposition

As reported in our earlier work [22], Cu–Al–Ni  $\beta$ -phase alloys undergo spinodal decomposition. The separation of NiAl phase from the  $\beta$ -phase occurs via the mechanism of spinodal decomposition. In our previous work only the bulk alloys were examined. Recently, we have carried out detailed investigation of these alloys prepared by a spin-quenching technique. The rapidly solidified alloys exhibit phase transformations similar to those in the bulk alloys. A represen-

tative micrograph and the corresponding diffraction pattern obtained from a rapidly solidified ribbon are shown in Fig. 4. A modulated structure can be seen in the dark-field image, and in the diffraction pattern the satellite spots are clearly visible. These features are typically associated with the structure produced by spinodal decomposition. Although the transformations leading to spinodal decomposition have been clearly demonstrated in the case of alloys containing 10 wt % Ni, the minimum concentration of nickel necessary for spinodal decomposition to occur has not yet been established. According to the vertical section of the Cu–Al–Ni phase diagram shown in Fig. 1, NiAl phase begins to appear when nickel exceeds about 5 wt %. It is probable, therefore, that spinodal decomposition occurs in alloys containing more than 5 wt % Ni. As reported earlier, a rapid increase in the intergranular embrittlement is observed when nickel exceeds 5 wt % [2].

Almost all the alloys undergoing spinodal decomposition in which fracture characteristics have been investigated show intergranular embrittlement. Alloy systems exemplifying such behaviour include Cu–Ni–Fe [23], Cu–Sn–Ni [24], Au–Pt [25], Al–Zn [26], etc. The extreme brittleness observed in high-nickel alloys (such as Cu–14 wt % Al–10 wt % Ni) may very well be related to spinodal decomposition. Various explanations have been given for the association of intergranular embrittlement with spinodal decomposition. A general result of spinodal decomposition is the hardening of the matrix [27], which would make stress relaxation at the grain boundaries difficult. Discontinuous coarsening of the spinodal structure [23] and precipitation at the grain boundaries [24] have been observed and correlated with the embrittlement. Two other factors which have not yet been investigated are the role of the enhanced modulus effect associated with modulated structures [28] and the role of the increase in elastic anisotropy of the matrix due to spinodal decomposition.

### 3.7. Grain size

A large grain size tends to promote intergranular fracture. The role of grain size may be especially significant in the case of ordered alloys undergoing

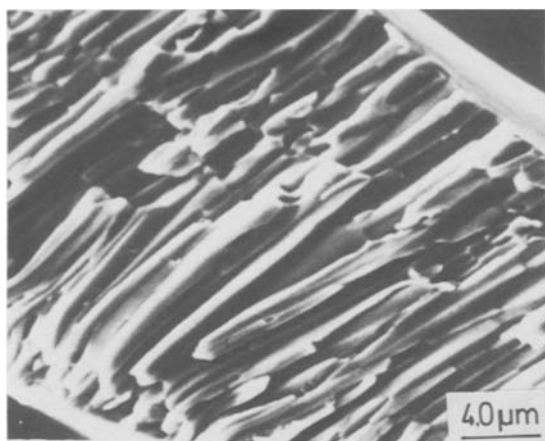


Figure 5 SEM image showing intergranular fracture observed in the columnar regions of rapidly solidified ribbons.

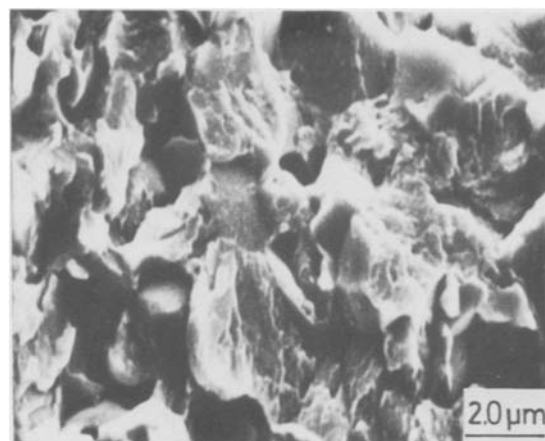


Figure 6 SEM image showing transgranular fracture observed in the regions having equiaxed grains.

spinodal decomposition. In this respect it would be interesting to analyse the theory put forward by Schulson [29]. After observing that the decrease in grain size decreases the tendency for intergranular fracture in many ordered alloys, Schulson proposed that a critical grain size exists below which a given material is ductile. The critical grain diameter is represented as

$$d_c = (YK_{IC} - k_y)/\sigma_i$$

where  $Y$  is a geometrical parameter close to unity,  $K_{IC}$  is the fracture toughness, and  $k_y$  and  $\sigma_i$  are the Hall and Petch parameters.

It should be noted that atomic ordering is known to cause a marked increase in  $k_y$  [30]. Thus ordered alloys may be expected to have much smaller values of  $d_c$ .

In order to study the role of grain size the fracture behaviour of spin-quenched ribbons was investigated. Whereas the average grain size in the bulk  $\beta$ -phase alloys ranges from 0.5 to 2 mm, the structure observed in the ribbons was much more refined. The grain structure was predominantly columnar, with the width varying from 1 to 4  $\mu\text{m}$  and the length from 5 to 20  $\mu\text{m}$ . Some regions had equiaxed grains varying in size from 1 to 5  $\mu\text{m}$ . When these ribbons were fractured by bending and examined using scanning electron microscopy, it was observed that the fracture is almost completely intergranular (Fig. 5). The regions having small equiaxed grains behaved differently and showed predominantly transgranular fracture (Fig. 6). These observations suggest that small grain size alone may not improve the fracture characteristics. The fracture behaviour would improve only if very small equiaxed grains were obtained.

#### 4. Conclusions

1. The intergranular embrittlement in Cu–Al–Ni  $\beta$ -phase alloys is not due either to grain boundary precipitates or to segregation of impurities at the grain boundaries. Intrinsic characteristics of these alloys appear to play a significant role in the embrittlement.

2. The grain size does not significantly affect the embrittlement characteristics of these alloys.

3. Severe embrittlement in high-nickel alloys ( $\text{Ni} >$

5 wt %) is associated with spinodal decomposition in these alloys.

#### Acknowledgements

The authors are grateful to Drs J. E. Morral, D. I. Potter and A. Tauqir of the Department of Metallurgy, University of Connecticut and Dr F. H. Hashmi of the Dr A. Q. Khan Research Laboratories for helpful discussions.

#### References

1. T. W. DUERIG, J. ALBRECHT and G. H. GESSINGER, *J. Metals* **35** (December 1982) 14.
2. S. W. HUSAIN and P. C. CLAPP, *J. Mater. Sci.* **22** (1987) 509.
3. W. O. ALEXANDER, *J. Inst. Metals* **63** (1938) 163.
4. S. W. HUSAIN and P. C. CLAPP, *J. Mater. Sci.* **22** (1987) 2351.
5. E. D. HONDROS and M. P. SEAH, *Int. Met. Rev.* **222** (1977) 262.
6. D. F. STEIN, W. C. JOHNSON and C. L. WHITE, in "Grain boundary structure and properties", edited by G. A. Chadwick and D. A. Smith (Academic, London, 1976) p. 301.
7. J. P. HIRTH, *Met. Trans.* **3** (1972) 3047.
8. C. ZENER, "Elasticity and Anelasticity of Metals" (University of Chicago Press, Chicago, 1948) p. 16.
9. M. SUEZAWA and K. SUMINO, *Scripta Metall.* **10** (1976) 789.
10. S. MIYAZAKI, T. KAWAI and K. OTSUKA, *ibid.* **16** (1982) 431.
11. R. VON MISES, *Z. Angew. Math. Mech.* **8** (1928) 161.
12. T. L. JOHNSTON, R. J. STOKES and C. H. LI, *Phil. Mag.* **7** (1962) 23.
13. A. BALL and R. E. SMALLMAN, *Acta Metall.* **14** (1966) 1517.
14. M. J. MARCINKOWSKI, in "Treatise on Materials Science and Technology", Vol. 5, edited by H. Herman (Academic, New York, 1974) p. 181.
15. C. H. LLOYD and M. H. LORETTO, *Phys. Status Solidi* **39** (1970) 163.
16. E. M. GRALA, in "Mechanical Properties of Intermetallic Compounds", edited by J. H. Westbrook (Wiley, New York, 1960) p. 358.
17. P. A. FLINN, *Trans. TMS-AIME* **218** (1960) 145.
18. J. H. WESTBROOK, in "Mechanical Properties of Intermetallic Compounds", edited by J. H. Westbrook (Wiley, New York, 1960) p. 1.
19. H. J. LEAMY and F. X. KAYSER, *Phys. Status Solidi* **34** (1969) 765.
20. M. J. MARCINKOWSKI and H. CHESSIN, *Phil. Mag.* **10** (1964) 837.

21. M. J. MARCINKOWSKI, *ibid.* **17** (1968) 159.
22. S. W. HUSAIN, P. C. CLAPP and M. AHMED, in Proceedings of International Conference on Phase Transformations in Solids, Greece, 1983 (Elsevier, New York, 1984) p. 729.
23. R. J. LIVAK and W. W. GERBERICH, in "Electron Microscopy and Structure of Materials", edited by G. Thomas (University of California Press, Berkeley, 1972) p. 647.
24. L. H. SCHWARTZ, S. MAHAJAN and J. T. PLEWES, *Acta Metall.* **22** (1974) 601.
25. R. W. CARPENTER, *ibid.* **15** (1967) 1297.
26. D. L. DOUGLASS and T. W. BARBEE, *J. Mater. Sci.* **4** (1969) 121.
27. M. KATO, T. MORI and L. H. SCHWARTZ, *Acta Metall.* **28** (1980) 285.
28. W. M. C. YANG, T. TSAKALAKOS and J. E. HILLIARD, *J. Appl. Phys.* **48** (1977) 876.
29. E. M. SCHULSON, *Res. Mech. Lett.* **1** (1981) 111.
30. M. J. MARCINKOWSKI and R. M. FISHER, *Trans. Met. Soc. AIME* **233** (1965) 293.

*Received 15 May  
and accepted 22 July 1987*